

Validation of the COSINE-100U NaI(Tl) Encapsulation for Low-Temperature Operation in Liquid Scintillator

K. Park^{*,1} S.-J. Cho,¹ L. E. França² C. Ha,³ J. Y. Kim,^{3,1} K. W. Kim,¹ S. H. Kim,¹ W. K. Kim,^{4,1} Y. J. Ko,⁵ D. H. Lee,^{6,1} H. S. Lee,^{1,4} I. S. Lee,¹ S. H. Lee,^{4,1} S. D. Park,^{6,1} G. H. Yu¹

¹*Center for Underground Physics (CUP), Institute for Basic Science (IBS), Daejeon 34126, Republic of Korea*

²*Physics Institute, University of São Paulo, São Paulo 05508-090, Brazil*

³*Department of Physics, Chung-Ang University, Seoul 06974, Republic of Korea*

⁴*IBS School, University of Science and Technology (UST), Daejeon 34126, Republic of Korea*

⁵*Department of Physics, Jeju National University, Jeju 63243, Republic of Korea*

⁶*Department of Physics, Kyungpook National University, Daegu 41566, Republic of Korea*

E-mail: kihong@ibs.re.kr, hyunsulee@ibs.re.kr

ABSTRACT: The COSINE-100U (upgrade) will enhance the sensitivity of the COSINE-100 dark matter search by operating the detector array immersed in liquid scintillator (LS) at -30°C . To validate the detector design for these conditions, we constructed a module using the COSINE-100U encapsulation and performed a dedicated long-term stability study. The module was first monitored at room temperature for \sim 110 days in air, followed by a one-week immersion in LAB-based LS to verify initial compatibility. Upon confirming stable optical performance, the temperature was lowered to -33°C . During approximately 150 days of continuous operation at low temperature, we observed no degradation in performance. These results demonstrate the chemical and mechanical robustness of the encapsulation, confirming its suitability for the COSINE-100U physics run.

KEYWORDS: Scintillators, dark matter detectors, Detector cooling and thermo-stabilization, Detector design and construction technologies and materials

Contents

1	Introduction	1
2	Experimental setup	2
3	Data analysis and results	4
3.1	Scintillation characteristics at room temperature and low temperature	4
3.1.1	Decay time measurement	4
3.1.2	Light yields	6
3.2	Stability of the detector encapsulation	6
4	Conclusions	8

1 Introduction

Astrophysical and cosmological observations consistently point to the presence of non-luminous matter that dominates the mass density of the Universe [1, 2]. The nature of this dark matter remains unknown, and several complementary strategies are pursued in parallel: direct searches with low-background underground detectors, indirect probes of annihilation or decay products, and collider-based searches for dark-sector states at electron–positron and hadron colliders [3–8].

Although no concrete evidence of dark matter interactions has yet been observed, there remains the long-standing debate surrounding DAMA/LIBRA, which reported a clear annual-modulation signal in a NaI(Tl) crystal array compatible with dark matter [9, 10]. The COSINE-100 experiment [11] was designed to test DAMA/LIBRA using the same target material and comparable analysis techniques. The experiment deployed eight low-background NaI(Tl) crystals, with a total mass of 106 kg, inside a liquid-scintillator veto [12] surrounded by copper, lead, and plastic scintillator muon panels [13] at the Yangyang underground laboratory in Korea. COSINE-100 has carried out both model-independent searches for a dark-matter–induced annual modulation [14–17] and model-dependent spectral analyses [18–20], finding no signals compatible with DAMA/LIBRA in NaI(Tl).

Beyond testing the DAMA/LIBRA claim, NaI(Tl) offers unique advantages due to the unpaired protons in both sodium and iodine isotopes. Given the relatively low mass number of sodium, NaI(Tl) has competitive sensitivity to Spin-Dependent WIMP-proton interactions in the low-mass dark matter region, as demonstrated in recent COSINE-100 results [20]. To further explore this parameter space, the COSINE-100 upgrade (COSINE-100U) [21] is being commissioned at Yemilab [22, 23], a new underground laboratory in Korea. This upgrade aims to enhance sensitivity to low-mass dark matter by increasing the light collection efficiency

A key feature of the upgrade is a novel crystal encapsulation technique [24]. Because NaI(Tl) is hygroscopic, crystals are typically encased in copper with a quartz optical window. To maximize

light yield, we developed an encapsulation method that couples photomultiplier tubes (PMTs) directly to the crystal, eliminating the quartz window. This design enhances light collection efficiency by approximately 50% [24, 25]. The long-term stability of this design in liquid scintillator (LS) at room temperature (RT) was previously demonstrated by the NEON experiment [26] over two years of operation [25].

While COSINE-100U has begun initial physics operations at Yemilab [22, 23] with crystals at RT, the ultimate goal is to operate the array at a low temperature (LT) of approximately -30°C [21]. This lower temperature offers the dual advantages of increased intrinsic light yield and improved pulse shape discrimination [27]. However, operating hygroscopic NaI(Tl) crystals immersed in LS at cryogenic temperatures introduces significant engineering challenges, specifically regarding the chemical compatibility of the encapsulation seals and the thermo-mechanical stress during cooling.

This work serves as the critical validation of the encapsulation design prior to the cryogenic deployment of the full COSINE-100U array. We present a dedicated long-term stability measurement of a NaI(Tl) crystal encapsulated using the COSINE-100U method. The detector was operated first at RT without LS, and then fully immersed in LS at -33°C . We monitored the light yield and energy resolution of the 59.54 keV γ -ray line from an ^{241}Am source throughout the study. We find that the optical quality of the NaI(Tl) crystal remained unchanged during an operation period of approximately one year, which included roughly 110 days at RT and 150 days at -33°C . These results validate the robustness of the COSINE-100U encapsulation for operation in LS at approximately -30°C .

2 Experimental setup

The prototype detector utilizes the NaI-037 NaI(Tl) crystal [28], grown at the Center for Underground Physics (IBS, Korea) using the purified powder described in Refs [29, 30]. The crystal is cylindrical, with a diameter of 70 mm and a height of 51 mm, and has a mass of approximately 0.70 kg after surface polishing.

We followed the encapsulation procedure developed for COSINE-100U [21], with one modification: the crystal edges were not machined, as the 70 mm diameter already matches the active area of the 3-inch PMTs. Prior to assembly, all encapsulation materials were cleaned in dilute Citranox via sonication, baked in an oven, and transferred to a glovebox. The glovebox atmosphere was maintained with a humidity (H_2O) level of $\mathcal{O}(10)$ ppm using a molecular-sieve trap. During the assembly, the glovebox was flushed with N_2 gas at a rate of 5 L/min to minimize ^{222}Rn contamination from component emanation. The crystal end faces were mirror-polished using a polishing pad with SiO_2 abrasives, while the barrel surface was gently wiped with anhydrous ethanol.

For the optical interface, 2 mm thick silicone pads (Eljen EJ-560) were coupled to the top and bottom faces of the crystal. Two high-quantum-efficiency 3-inch PMTs (Hamamatsu R12669SEL) were attached to these pads to maximize light collection. The curved side of the crystal was wrapped in several layers of soft, Polytetrafluoroethylene (PTFE)-based Tetratex, which serves as a diffuse reflector to contain scintillation light. A PTFE holder secures the mechanical coupling between the crystal and PMTs, ensuring uniform optical contact. The entire assembly was centered in a copper support and enclosed in a copper housing matching the COSINE-100U design [21]. Crucially,

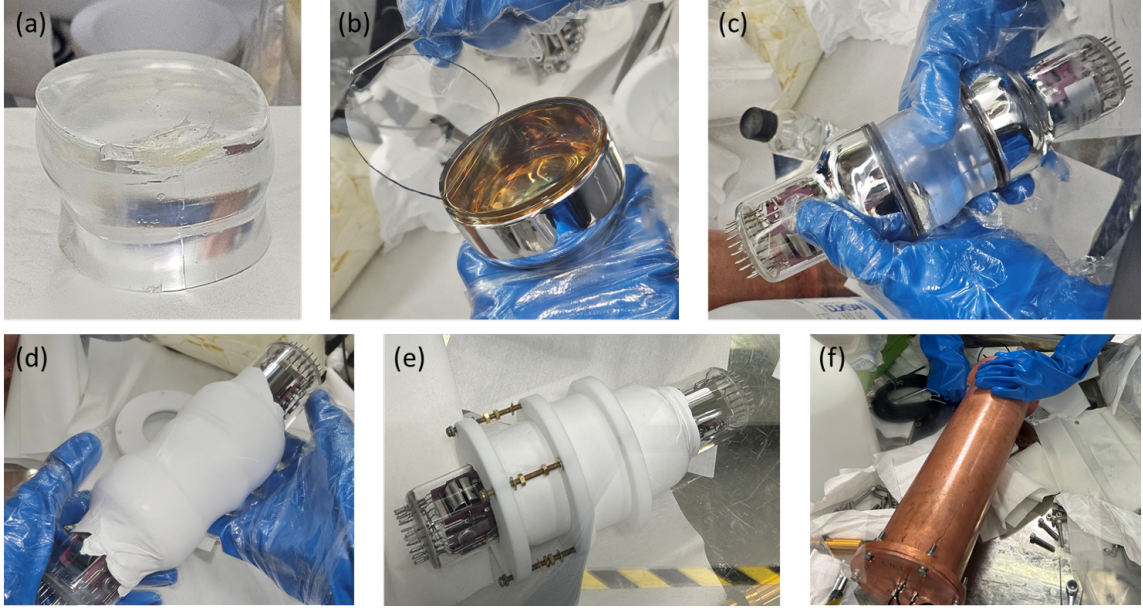


Figure 1: Assembly sequence of the NaI-037 NaI(Tl) detector: (a) the polished crystal after surface treatment; (b) attachment of the silicone optical pad to the PMT window; (c) the crystal coupled to two 3-inch Hamamatsu R12669SEL PMTs; (d) wrapping of the crystal and PMT assembly with PTFE-based Tetratex reflector; (e) installation of the PTFE holder to secure the crystal and PMTs; and (f) insertion of the assembled detector into the upgraded COSINE-100U copper housing.

the housing is sealed using Viton O-rings selected for their chemical compatibility with LS and mechanical resilience at -30°C . The overall assembly procedure is illustrated in Fig. 1.

The stability of this encapsulation design in LS at RT was previously demonstrated by the NEON experiment over a two-year period [25]. Therefore, we first operated the detector in an ambient air environment at RT to verify the seal integrity against humidity. Since NaI(Tl) is hygroscopic, any ingress of ambient air would degrade the crystal surface and reduce the light yield. As shown in Fig. 2 (a), the detector was shielded by 10 cm of lead to reduce external background radiation.

After approximately 110 days of stable operation in air, the detector was immersed in LS to prepare for low-temperature testing. Following a one-week stability check in LS at RT, the setup was transitioned to low-temperature operation. The detector and LS volume were placed in a plastic container inside a commercial chest refrigerator, as shown in Fig. 2 (b). To stress-test the encapsulation against thermal shock, the refrigerator was set directly to its minimum temperature without a gradual cooling ramp. The equilibrium temperature was measured at -33°C , sufficient to validate the design for the planned -30°C operation of COSINE-100U. The detector was then operated under these conditions for approximately 150 days to monitor long-term stability.

Signals from the PMTs were amplified by custom-built preamplifiers and digitized by a 500 MHz, 12-bit flash analog-to-digital converter. A trigger was generated when a signal corresponding to one or more photoelectrons occurred in each PMT within a 200 ns coincidence window. For RT data, an $8\ \mu\text{s}$ waveform (starting $2.4\ \mu\text{s}$ before the trigger) was recorded. For low-temperature operation, the recording window was extended to $16\ \mu\text{s}$ to account for the increased scintillation decay time of

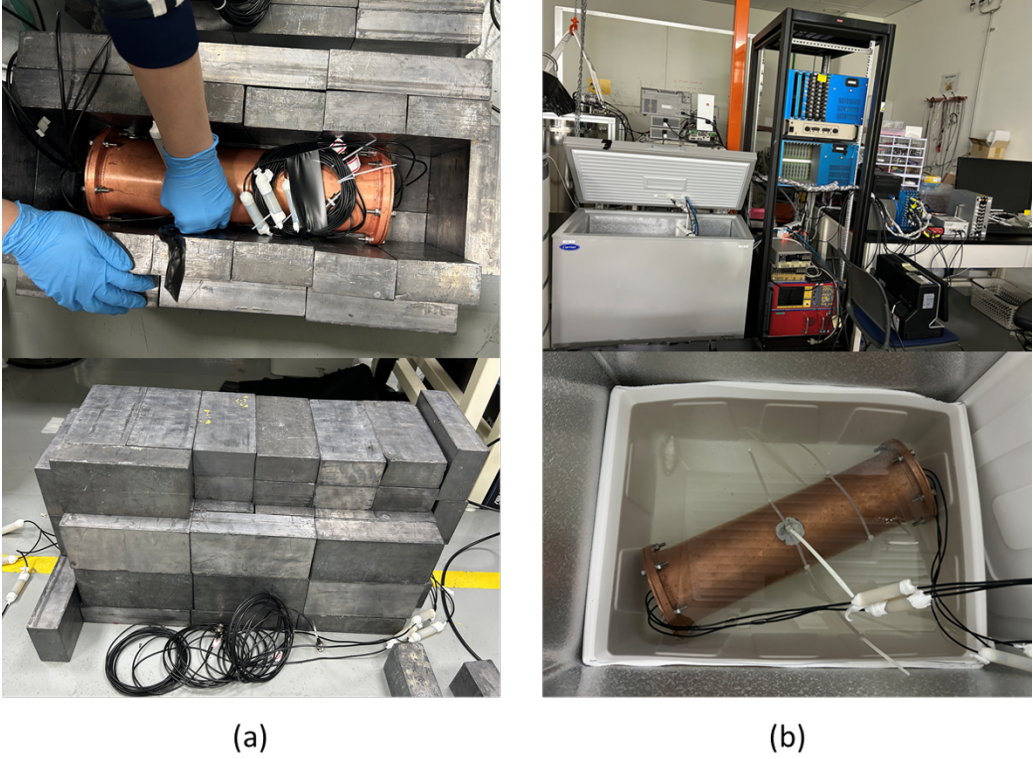


Figure 2: Photographs of the NaI-037 experimental setup. (a) Room temperature configuration: the encapsulated detector placed inside the lead shielding (top) and the lead bricks surrounding the setup (bottom). (b) Low-temperature configuration: the DAQ rack and refrigerator used for measurements (top) and the NaI-037 detector immersed in LS inside the refrigerator at -33°C (bottom).

NaI(Tl) at -33°C [27]. Data were transferred to a Linux computer via USB-3 and stored using a ROOT [31]-based data acquisition software similar to the COSINE-100 DAQ system [32].

The detector response was calibrated using 59.54 keV γ -rays from an ^{241}Am source. To ensure the consistency of the long-term stability measurement, the source was maintained in a fixed position relative to the crystal throughout the entire campaign, eliminating systematic uncertainties related to position dependence.

3 Data analysis and results

3.1 Scintillation characteristics at room temperature and low temperature

3.1.1 Decay time measurement

The scintillation decay time directly influences the optimization of the integration window, the pile-up probability, and the efficiency of pulse-shape-based background rejection. To quantify these effects, we compared the scintillation decay times of 59.54 keV γ -ray events from an ^{241}Am source at RT and at -33°C .

For a precise comparison, we constructed accumulated waveforms of the 59.54 keV peak events for both temperatures, as shown in Fig. 3. At RT, the waveform is well-described by a two-component

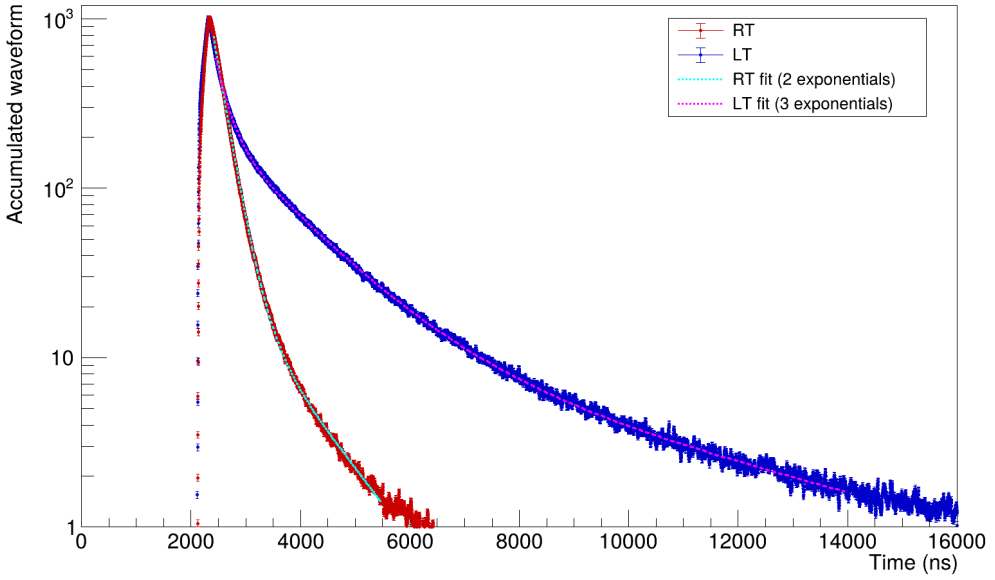


Figure 3: Accumulated waveforms for 59.54 keV events from an ^{241}Am source at room temperature (RT) and -33°C (LT), with the corresponding best-fit multi-exponential models overlaid. The extended tail observed at -33°C reflects the increased contribution of the intermediate and slow decay components.

exponential model [27]:

$$V_{\text{RT}}(t) = A_1 e^{-(t-t_0)/\tau_1} + A_2 e^{-(t-t_0)/\tau_2}, \quad (3.1)$$

where τ_1 and τ_2 denote the fast and slow decay constants, and A_1 and A_2 are the corresponding amplitudes.

At -33°C , the same two-component model failed to adequately describe the waveform, particularly the extended decay tail. Consequently, we introduced a three-component model [33]:

$$V_{\text{LT}}(t) = B_1 e^{-(t-t_0)/\tau_1} + B_2 e^{-(t-t_0)/\tau_2} + B_3 e^{-(t-t_0)/\tau_3}, \quad (3.2)$$

where τ_1 , τ_2 , and τ_3 represent the fast, intermediate, and slow decay constants, respectively, and B_1 , B_2 , and B_3 are the corresponding amplitudes. We fitted the accumulated data for both room-temperature and low-temperature configurations using these functions, as illustrated in Fig. 3.

The extracted decay constants and component fractions are summarized in Table 1. The fast decay constant (τ_1) remains consistent at approximately 200 ns at both temperatures. The intermediate decay constant (τ_2) is also stable, with a value on the order of 1000 ns. However, the low-temperature waveform exhibits an additional slow component (τ_3) on the order of 5000 ns. Notably, the contribution of the fast component decreases dramatically from 89% at RT to 29% at -33°C .

At lower temperatures, non-radiative quenching channels are suppressed, and a larger fraction of excitations are delayed in trapping states before reaching the Tl activator sites [27, 34, 35]. This results in a redistribution of scintillation light into the intermediate and slow components, leading to

Table 1: Fitted decay constants and component fractions (f_1 and f_2) for the multi-exponential model applied to accumulated ^{241}Am 59.54 keV waveforms at room temperature and -33°C . At room temperature, a two-exponential model provides an adequate description, so no τ_3 parameter is included. At -33°C , a three-exponential model is used. Quoted uncertainties are statistical and rounded to one decimal place.

Temperature	τ_1 [ns]	τ_2 [ns]	τ_3 [ns]	f_1 [%]	f_2 [%]
Room temp.	220.4 ± 0.6	1030.0 ± 4.3	–	88.8 ± 0.1	11.2 ± 0.1
-33°C	208.9 ± 2.4	1244.1 ± 4.7	5048.8 ± 29.6	29.4 ± 0.4	54.5 ± 0.2

Table 2: Light yield and energy resolution for the ^{241}Am 59.54 keV peak measured at room temperature and -33°C

Temperature	Window [μs]	Light yield [PEs/keV]	Resolution [%]
Room temp.	8	21.9 ± 0.2	4.02 ± 0.15
-33°C	16	23.2 ± 0.2	3.66 ± 0.13

an overall longer decay time at -33°C . This behavior necessitates a longer integration window for low-temperature operation and suggests that pulse-shape discrimination techniques may benefit from the enhanced separation between fast and slow components in the COSINE-100U environment.

3.1.2 Light yields

The single-photoelectron charge distribution is constructed from the charges of individual isolated clusters identified in the decay tail of the waveforms [36]. These cluster charges are fitted with a model consisting of a Poisson signal component and an exponential background. The light yield of the detector is determined by comparing the mean charge of the 59.54 keV peak to the mean single-photoelectron charge. The energy resolution is defined as the ratio σ/μ , where σ and μ correspond to the root-mean-square and mean, respectively, of the 59.54 keV γ -ray charge distribution.

The measured light yield and energy resolution for the 59.54 keV line at RT and -33°C are summarized in Table 2. At RT, we measured a high light yield of 21.9 ± 0.2 photoelectrons/keV (PEs/keV). At LT, this value increased to 23.2 ± 0.2 PEs/keV. Correspondingly, the energy resolution improved from $4.02 \pm 0.15\%$ to $3.66 \pm 0.13\%$, a performance enhancement consistent with previous low-temperature studies [27].

3.2 Stability of the detector encapsulation

We evaluated the long-term stability of the NaI-037 light yield through frequent monitoring of the 59.54 keV γ -ray peak. The monitoring campaign began in December 2024 with the detector operating in air at RT, utilizing the setup described in Fig. 2 (a). This phase continued until March 2025, after which the detector remained in ambient air conditions until June 2025. This initial period served to verify the mechanical air-tightness of the seal against ambient humidity.

In June 2025, the detector was immersed in LAB-based LS as shown in Fig. 2 (b). We first performed a one-week stability check in LS at RT to ensure no immediate chemical interaction

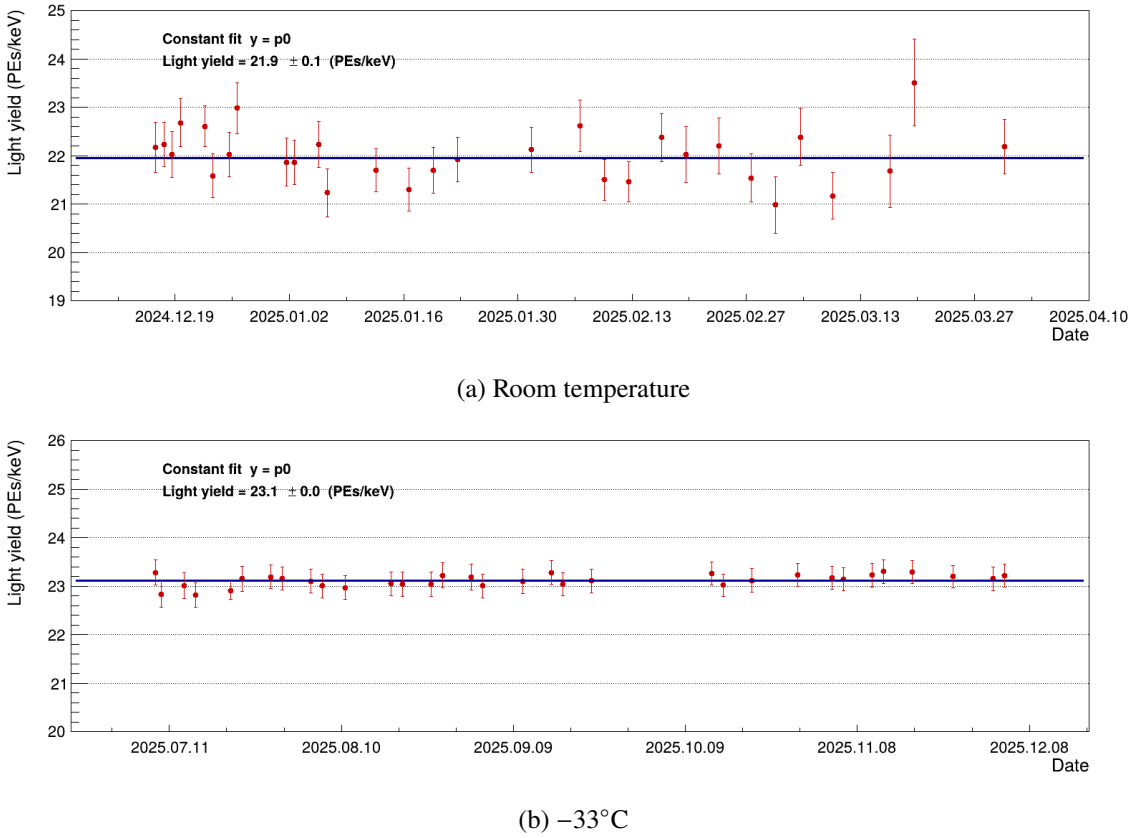


Figure 4: Light yield monitoring of the NaI-037 detector. (a) Time evolution of the light yield at room temperature in ambient air conditions. (b) Time evolution of the light yield at -33°C while immersed in LS. The solid lines represent fits to a constant function. The consistent light yield observed throughout the measurement periods demonstrates that the COSINE-100U encapsulation is sufficiently stable to maintain optical performance during long-term operation in LS at -30°C .

or leakage occurred at the O-ring interface. Following this confirmation, the refrigerator was switched on and set directly to its minimum temperature to simulate a rapid cool-down scenario. We allowed approximately one week for the system to reach a stable thermal equilibrium at -33°C . The low-temperature measurement phase spanned approximately 150 days, from July 2025 to December 2025, representing the critical validation period for the upgrade.

Figure 4 illustrates the temporal evolution of the measured light yield for the room-temperature (a) and -33°C (b) periods. The data points show excellent agreement with a constant light yield model. For the room-temperature phase, we measured a mean light yield of 21.94 ± 0.09 PEs/keV. For the crucial low-temperature phase in LS, the mean light yield was 23.11 ± 0.04 PEs/keV. The stability of these values confirms that the detector response is time-independent.

To quantitatively bound any potential degradation, we also fitted the data with a linear function ($y = p_0 + p_1 x$). The slope parameter p_1 provides an upper limit on the degradation rate. We obtained a value of $p_1 = (1.5 \pm 0.9) \times 10^{-3}$ PEs/keV/day for -33°C , which is consistent with zero within statistical uncertainties. This measurement effectively rules out common failure modes associated

with LS immersion, such as the infiltration of LS into the PTFE reflector (which would reduce reflectivity) or the clouding of the crystal surface due to chemical ingress. Furthermore, the stability at -33°C confirms that the silicone optical pads maintained robust coupling to the crystal and PMTs despite the differential thermal contraction of the assembly.

Crucially, the stable operation in LS at -33°C for approximately 150 days provides strong evidence for the robustness of the COSINE-100U encapsulation. This result validates the engineering design for the full experiment’s physics run at -30°C , which is scheduled to commence in March 2026.

4 Conclusions

We have successfully validated the performance and long-term stability of the COSINE-100U encapsulation design using the prototype NaI-037 detector. This study serves as a critical engineering pre-test for the experiment’s upgrade, specifically targeting the challenges of operating hygroscopic NaI(Tl) crystals immersed in LS at cryogenic temperatures.

The detector exhibited robust performance across all testing phases. During the initial 100-day operation in air at RT, the light yield remained stable, confirming the mechanical integrity of the seals against ambient humidity. Following immersion in LS and a rapid cool-down to -33°C , the detector maintained stable performance over a 150-day monitoring period. A linear fit to the light yield data during this phase is consistent with zero degradation, effectively ruling out chemical incompatibility with the LS or mechanical decoupling due to thermal stress.

In addition to demonstrating stability, the low-temperature operation provided clear performance benefits. At -33°C , we observed a relative increase in light yield of approximately 5.6% and an improvement in 59.54 keV energy resolution of approximately 9% compared to RT. Analysis of the accumulated waveforms confirmed the expected increase in the scintillation decay time at LT, necessitating the extension of the integration window to $16\ \mu\text{s}$.

In summary, these results demonstrate that the upgraded encapsulation ensures chemical and mechanical robustness under the target operating conditions of COSINE-100U. With the stability of the design verified, the COSINE-100U experiment is on schedule to commence its physics run at -30°C in March 2026, with enhanced sensitivity to low-mass dark matter.

Acknowledgments

This work is supported by the Institute for Basic Science (IBS) under project code IBS-R016-A1, NRF-2021R1A2C3010989, NRF-2021R1A2C1013761, RS-2024-00356960, RS-2025-25442707 and RS-2025-16064659, Republic of Korea; Grant No. 2022/13293-5 and 2025/01639-2 FAPESP, CNPq 304658/2023-5, Brazil.

References

- [1] G. Bertone, D. Hooper and J. Silk, *Particle dark matter: Evidence, candidates and constraints*, *Phys. Rept.* **405** (2005) 279 [[hep-ph/0404175](#)].
- [2] G. Bertone and D. Hooper, *History of dark matter*, *Rev. Mod. Phys.* **90** (2018) 045002 [[1605.04909](#)].

- [3] L. Baudis, *Direct dark matter detection: the next decade*, *Phys. Dark Univ.* **1** (2012) 94 [[1211.7222](#)].
- [4] J. Conrad and O. Reimer, *Indirect dark matter searches in gamma and cosmic rays*, *Nature Phys.* **13** (2017) 224 [[1705.11165](#)].
- [5] J. Abdallah et al., *Simplified Models for Dark Matter Searches at the LHC*, *Phys. Dark Univ.* **9-10** (2015) 8 [[1506.03116](#)].
- [6] D. Abercrombie et al., *Dark Matter benchmark models for early LHC Run-2 Searches: Report of the ATLAS/CMS Dark Matter Forum*, *Phys. Dark Univ.* **27** (2020) 100371 [[1507.00966](#)].
- [7] K. Park, K. Kim, A. Sytov and K. Cho, *Search for Dark Photon in $e^+e^- \rightarrow A'A'$ Using Future Collider Experiments*, *J. Astron. Space Sci.* **40** (2023) 259.
- [8] K. Park, K. Kim, A. Sytov and K. Cho, *Study of dark photons using future electron–positron colliders based on machine learning*, *J. Korean Phys. Soc.* **84** (2024) 403.
- [9] R. Bernabei et al., *Final model independent result of DAMA/LIBRA-phase1*, *Eur. Phys. J. C* **73** (2013) 2648 [[1308.5109](#)].
- [10] R. Bernabei et al., *First model independent results from DAMA/LIBRA-phase2*, *Nucl. Phys. Atom. Energy* **19** (2018) 307 [[1805.10486](#)].
- [11] G. Adhikari et al., *Initial Performance of the COSINE-100 Experiment*, *Eur. Phys. J. C* **78** (2018) 107 [[1710.05299](#)].
- [12] G. Adhikari et al., *The COSINE-100 liquid scintillator veto system*, *Nucl. Instrum. Meth. A* **1006** (2021) 165431 [[2004.03463](#)].
- [13] COSINE-100 collaboration, *Muon detector for the COSINE-100 experiment*, *JINST* **13** (2018) T02007 [[1712.02011](#)].
- [14] COSINE-100 collaboration, *Search for a dark matter-induced annual modulation signal in NaI(Tl) with the COSINE-100 Experiment*, *Phys. Rev. Lett.* **123** (2019) 031302 [[1903.10098](#)].
- [15] COSINE-100 collaboration, *Three-year annual modulation search with COSINE-100*, *Phys. Rev. D* **106** (2022) 052005 [[2111.08863](#)].
- [16] COSINE-100 collaboration, *COSINE-100 full dataset challenges the annual modulation signal of DAMA/LIBRA*, *Sci. Adv.* **11** (2025) adv6503 [[2409.13226](#)].
- [17] ANAIS-112, COSINE-100 collaboration, *Combined Annual Modulation Dark Matter Search with COSINE-100 and ANAIS-112*, *Phys. Rev. Lett.* **135** (2025) 121002 [[2503.19559](#)].
- [18] G. Adhikari et al., *An experiment to search for dark-matter interactions using sodium iodide detectors*, *Nature* **564** (2018) 83 [[1906.01791](#)].
- [19] COSINE-100 collaboration, *Strong constraints from COSINE-100 on the DAMA dark matter results using the same sodium iodide target*, *Sci. Adv.* **7** (2021) abk2699 [[2104.03537](#)].
- [20] COSINE-100 collaboration, *Limits on WIMP Dark Matter with NaI(Tl) Crystals in Three Years of COSINE-100 Data*, *Phys. Rev. Lett.* **135** (2025) 231001 [[2501.13665](#)].
- [21] D. Lee et al., *Upgrading the COSINE-100 experiment for enhanced sensitivity to low-mass dark matter detection*, *Commun. Phys.* **8** (2025) 135 [[2409.15748](#)].
- [22] K.S. Park, Y.D. Kim, K.M. Bang, H.K. Park, M.H. Lee, J. So et al., *Construction of Yemilab*, *Front. in Phys.* **12** (2024) 1323991 [[2402.13708](#)].
- [23] Y. Kim and H.S. Lee, *Yemilab, a new underground laboratory in Korea*, *AAPPS Bull.* **34** (2024) 25.

[24] J.J. Choi, B.J. Park, C. Ha, K.W. Kim, S.K. Kim, Y.D. Kim et al., *Improving the light collection using a new NaI(Tl) crystal encapsulation*, *Nucl. Instrum. Meth. A* **981** (2020) 164556 [[2006.02573](#)].

[25] NEON collaboration, *Upgrade of the NaI(Tl) crystal encapsulation for the NEON experiment*, *JINST* **19** (2024) P10020 [[2404.03691](#)].

[26] NEON collaboration, *Exploring coherent elastic neutrino-nucleus scattering using reactor electron antineutrinos in the NEON experiment*, *Eur. Phys. J. C* **83** (2023) 226 [[2204.06318](#)].

[27] S.H. Lee, G.S. Kim, H.J. Kim, K.W. Kim, J.Y. Lee and H.S. Lee, *Study on NaI(Tl) crystal at -35°C for dark matter detection*, *Astropart. Phys.* **141** (2022) 102709 [[2111.03328](#)].

[28] H. Lee et al., *Performance of an ultra-pure NaI(Tl) detector produced by an indigenously-developed purification method and crystal growth for the COSINE-200 experiment*, *Front. in Phys.* **11** (2023) 1142765 [[2301.04884](#)].

[29] K. Shin, O. Gileva, Y. Kim, H.S. Lee and H. Park, *Reduction of the radioactivity in sodium iodide (NaI) powder by recrystallization method*, *J. Radioanal. Nucl. Chem.* **317** (2018) 1329.

[30] K. Shin, J. Choe, O. Gileva, A. Iltis, Y. Kim, Y. Kim et al., *Mass production of ultra-pure NaI powder for COSINE-200*, *Front. in Phys.* **11** (2023) 1142849 [[2301.05400](#)].

[31] R. Brun and F. Rademakers, *ROOT — An object oriented data analysis framework*, *Nucl. Instrum. Meth. A* **389** (1997) 81.

[32] COSINE-100 collaboration, *The COSINE-100 Data Acquisition System*, *JINST* **13** (2018) P09006 [[1806.09788](#)].

[33] S.D. Park, J. Lee, H.S. Lee and H.J. Kim, *Investigation of scintillation properties of a CsI(Tl) crystal at low temperature for dark matter search*, *JINST* **19** (2024) P07011.

[34] H.Y. Lee, J.A. Jeon, K.W. Kim, W.K. Kim, H.S. Lee and M.H. Lee, *Scintillation characteristics of a NaI(Tl) crystal at low-temperature with silicon photomultiplier*, *JINST* **17** (2022) P02027 [[2110.03306](#)].

[35] C. Sailer, B. Lubsandozhiev, C. Strandhagen and J. Jochum, *Low temperature light yield measurements in NaI and NaI(Tl)*, *Eur. Phys. J. C* **72** (2012) 2061 [[1203.1172](#)].

[36] KIMS collaboration, *First limit on wimp cross section with low background csi(tl) crystal detector*, *Phys. Lett. B* **633** (2006) 201 [[astro-ph/0509080](#)].